

IMPACT OF REDUCED SINTERING TEMPERATURE ON THE GRAIN SIZE OF SAMARIUM DOPED CERIA ELECTROLYTE

Sandhya K¹, Chitra Priya N S², Aswathy P K³, Deepthi N Rajendran⁴

Department of Physics, Govt. College for Women, University of Kerala, Thiruvananthapuram

Abstract

Synthesis of nanocrystalline electrolyte for industrial usage demand a deep understanding of ionic conductivity of the prepared material. Ionic conductivity mainly depends on the correlation between sintering temperature and the grain size of the nanocrystalline electrolyte. Therefore, the structural and electrical properties of nanocrystalline electrolyte have to be carefully investigated for solid oxide fuel applications. In the present work, $\text{Ce}_{0.8}\text{Sm}_{0.1}\text{Bi}_{0.1}\text{O}_2$ nanocrystalline were prepared by citrate gel method. XRD pattern confirm the fluorite structure with high crystallinity. Surface morphology were analyzed by scanning electron microscope. Electrochemical Impedance analysis helps to determine the frequency dependence of dielectric properties AC Conductivity value obtained at 1 MHz are suitable for solid oxide fuel cell applications.

Keywords: *Electrolyte, Citrate gel, AC Conductivity.*

I. INTRODUCTION

The trivalent rare earth doped ceria is generating enormous worldwide interest as electrolyte in solid oxide fuel cell (SOFC) [1]. SOFC operating temperature and efficiency depends on the oxy-ion conducting capability of the electrolyte. In other words, the highly desirable feature of an electrolyte fast oxygen ion transfer at reduced temperature. The main challenge before R & D is development of new oxy-ion conductors or optimization of the existing electrolyte to operate intermediate temperature SOFC applications with high ionic conductivity [2]. From the literature, it is noted the nanocrystalline material exhibit better electrical properties compared to microcrystalline one. Literature review on various trivalent rare earth doped ceria reports samarium doped ceria has the highest electrical conductivity [3]. Nanocrystalline samarium doped ceria offers faster densification kinetics, finer microstructure and more homogenous properties of the sintered materials.

Co-doping is reported to provide better ionic conductivity in nowadays. In the present work, bismuth co-doped samarium ceria oxide powder prepared by citrate gel method. The main attempt was made to investigate the ionic conductivity of the nanostructured Bismuth co-doped samarium ceria oxide powder with bismuth as co-dopant in the composition. The results of analysis notify that codoping resulted in enhanced ionic conductivity.

II. EXPERIMENTAL

Citrate gel method was used to prepare Bismuth co-doped samarium ceria oxide powder ($\text{Ce}_{0.8}\text{Sm}_{0.1}\text{Bi}_{0.1}\text{O}_{2-\delta}$) powder. In this method, analytical grade stoichiometric calculated amount of cerium nitrate ($\text{Ce}(\text{NO}_3)_3 \cdot 6\text{H}_2\text{O}$),

samarium nitrate ($\text{Sm}(\text{NO}_3)_3 \cdot 6\text{H}_2\text{O}$), bismuth nitrate ($\text{Bi}(\text{NO}_3)_3 \cdot 5\text{H}_2\text{O}$) were used as the sources of Ce, Sm and Bi components, and citric acid were chosen for the polymerization treatment. A white coloured gel precursors was formed and dried at 100°C for 6 h. The so-prepared amorphous precursors got converted into crystalline bismuth co-doped samarium ceria oxide powder by heating at 400°C for 2h. The calcinated powder were using hydraulic press by applying 2.5MPa pressure. The pellets were sintered at 600°C for 4h.

X-ray powder diffraction analysis were carried out XPERTO diffractometer by passing $\text{Cu- K}\alpha_1$ radiations of wavelength 1.54060\AA to determine the crystal structure and phase formation of the prepared powder. FTIR spectroscopy, IR Prestige-21 instrument used to obtain the composition of the prepared powder. Archimedes method were employed to evaluate the density of the sintered pellet by comparing with the theoretical density. Scanning Electron Microscopy images visualizes density, the surface smoothness, porosity, grain growth and shape of the sintered pellets. The electrochemical studies were obtained using Impedance analyser, Solatron 1250.

III. RESULTS AND DISCUSSIONS

3.1 X-RAY Diffraction Studies

Fig 1. symbolize the XRD pattern of $\text{Ce}_{0.8}\text{Sm}_{0.1}\text{Bi}_{0.1}\text{O}_{2-\delta}$ nanoparticle in which intensity is plotted as a function of angle 2θ over a range 20° to 90° . XRD pattern of as prepared sample matches with standard cubic fluorite structure ((JCPDS Card No. 34-0394) which indicate the complete dissolution of dopants into the CeO_2 lattice. Inter planar spacing(d) are obtained from the location of the most prominent peaks of the bragg's line. The crystallite size is evaluated using Scherrer equation

$$D = K\lambda/\beta \cdot \cos\theta \quad (1)$$

where D is crystallite size, K the Scherrer constant (0.94), λ the X-ray wavelength, β the full-width at half-maximum (FWHM) and θ the Bragg angle [4]. The calculated crystallite size and lattice parameter are shown in the table. It is noteworthy to point out that the no secondary phases of other crystalline phases or impurities appeared in the XRD pattern which approves $\text{Ce}_{0.8}\text{Sm}_{0.1}\text{Bi}_{0.1}\text{O}_{2-\delta}$ nanoparticle are highly pure in phase.

$\text{Ce}_{0.8}\text{Sm}_{0.1}\text{Bi}_{0.1}\text{O}_{2-\delta}$ display better ionic conductivity at intermediate temperature due to the increase in lattice parameter or decrease in crystallite size.

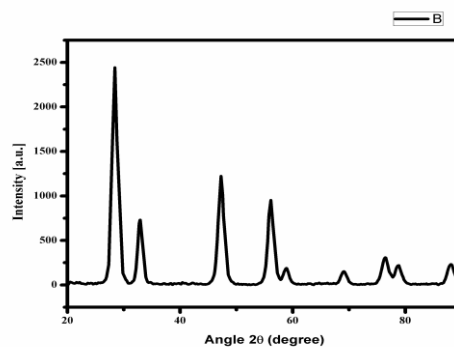


Fig. 1 The XRD Pattern of (B). $\text{Ce}_{0.8}\text{Sm}_{0.1}\text{Bi}_{0.1}\text{O}_{2-\delta}$ electrolyte

The Williamson–Hall (W–H) plot are between $\beta \cos\theta$ vs. $4 \sin\theta$ to determine crystalline size and lattice strain using the relation

$$\beta \cos\theta = 0.9\lambda / D + 4\epsilon \sin\theta \quad (2)$$

Title of figure centered, bold subsequent text Indented, Times New Roman 8, single line spacing

where slope of the straight line offers micro-strain while crystallite size is associated with the intercept parameter [5]. This computes relationship between ‘ ϵ ’ and ‘D’ values. The results given in the table indicate lattice strain is very small. Ionic conductivity depends upon the value of lattice strain. Lower lattice strain value indicates better ionic conductivity.

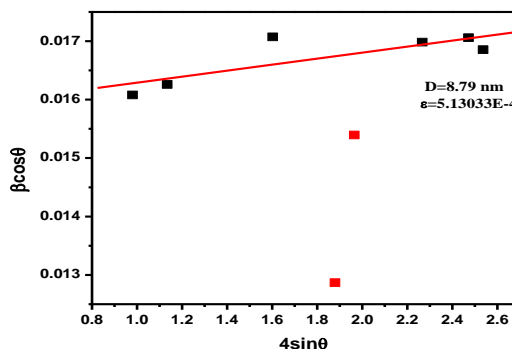


Fig 2. HW plot of (B). $Ce_{0.8}Sm_{0.1}Bi_{0.1}O_{2-\delta}$ electrolyte

Table 1: Data on Structural Properties of the prepared Electrolyte

Data	Parameter
D' (nm)	8.67nm
a (Å)	5,44179
FWHM(β_{avg})	.962
D(nm) from W-H plot	8.79 nm
Strain from W-H plot	5.1303E-4

3.3.FOURIER TRANSFORM INFRARED SPECTROSCOPY

IR Spectrum check up on the purity and composition of the prepared of the $Ce_{0.8}Sm_{0.1}Bi_{0.1}O_{2-\delta}$ nanoparticle [6]. Figure 3 illustrate IR Spectrum of the nanoparticle attained in the range 400 to 4000 cm^{-1} . From the spectrum it can be seen various vibrational modes of different groups present on the surface on the sample. The more intense and broad peak at 840 cm^{-1} portrait the stretching of Bi-O band. The stretching of O-H band is more specific in the range 3438 and 2075 cm^{-1} . The stretching of carbonyl containing function groups are noted as fine and broad peak at 1629 cm^{-1} . Ce-O band vibrations are noted in the band range 600 cm^{-1} and 800 cm^{-1} .

Shaper bands in the spectrum pomp’s the purity of the prepared sample.

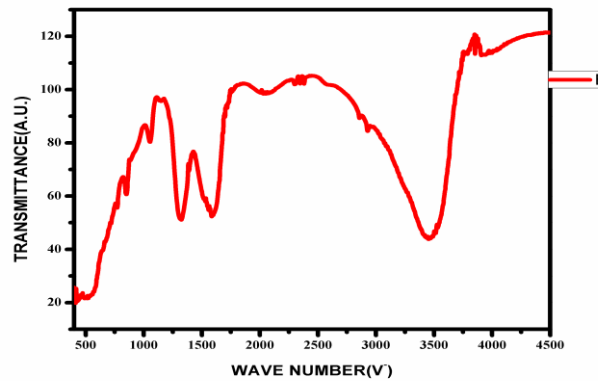


FIG 3: FTIR Spectra (B). $Ce_{0.8}Sm_{0.1}Bi_{0.1}O_{2-\delta}$ electrolyte

3.4 .Scanning Electron Microscopy Studies

The FE-SEM images of the sintered sample are shown in the figure. Round shape grains are noted in the figure. Average grains are calculated to be of the order using the linear intercept method given by

$$G = 1.5L/MN \quad (3)$$

Where L is the total test line length, M is the magnification and N is the total number of intercepts that the grain boundary makes with the line [7-8]. Narrow particle distribution with tightly packed surfaces enhances efficient charge carrier separation of the porous structure

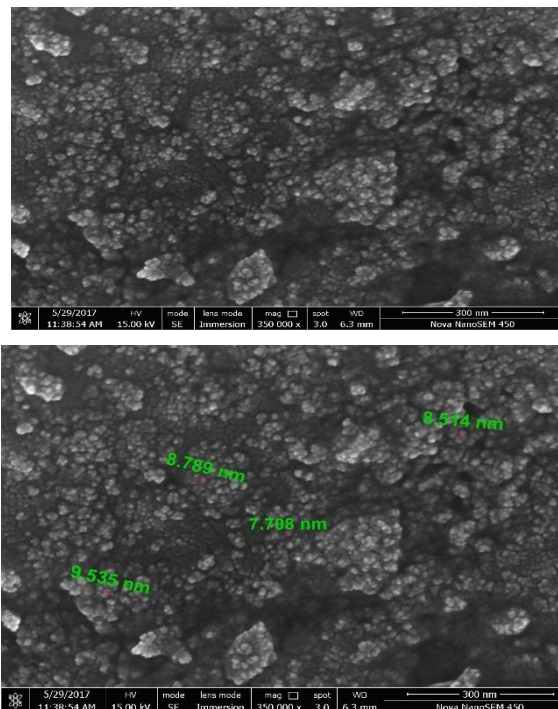


Fig.4.Scanning Electron Micrographs of $Ce_{0.8}Sm_{0.1}Bi_{0.1}O_{2-\delta}$ electrolyte

3.5. Electrical Studies

The fig 5 shows the Arrhenius plot of the doped electrolyte. The activation energy is evaluated from the plot of $\log \sigma$ versus $1000/T$ in the temperature 200-500°C. These plot shows curvature near temperature which divides the plot into two specific region There is a remarkable change in the activation energy of oxygen vacancy at low and high temperature [9-11]. This is mainly due to the interaction of defect with dopant. The ionic conductivity. The temperature dependence on the conductivity was evaluated using equation

$$\sigma = \sigma_0 \exp\left(-\frac{E_A}{kT}\right) \quad (4)$$

Here σ_0 is the high temperature limit of conductivity, E_A is activation energy and kT is associated with temperature variation in the measurement where k is Boltzmann constant and T is temperature [12-15]. The bulk activation energy for Bi doped SDC is calculated from the slope of Arrhenius plot and is .599 eV.

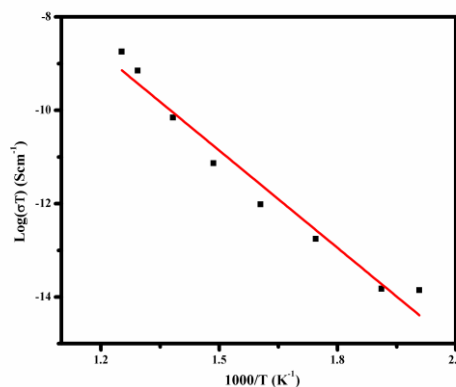


Fig 5. Arrhenius Plot of $Ce_{0.8}Sm_{0.1}Bi_{0.1}O_{2.6}$ prepared by citrate gel method

IV. CONCLUSION

Citrate gel method was used to prepare $Ce_{0.8}Gd_{0.1}Bi_{0.1}O_{2.6}$ nanopowder. The calculated crystallite size is 8.67 nm with high crystallinity. The XRD analysis confirm the formation of single phase cubic fluorite structure. The sintered pellet has round shape grain of size in the order of 9.35 nm. Arrhenius plot are drawn for various temperature and the electrical conductivity was found to be $1.27 \times 10^{-4} \text{ Scm}^{-1}$ at 500°C. It is marked that bismuth is a low melting point trivalent dopant, it can be sintered at smaller temperature along with the creation of more oxygen vacancies. The achieved electrical conductivity is suitable for solid oxide fuel cell applications

V. ACKNOWLEDGMENTS

The authors are express gratitude towards the University of Kerala for providing research facilities and for financial support as a University Junior Research Fellowship. We are also grateful to STIC Cochin and NIIIST Trivandrum for providing characterization facilities.

REFERENCES

[1].Gihyun Kim, Naesung Lee et.al, Int. J. Hyd.Ene. 38, pp. 1571-1587,(2013) .

- [2].M. Prekajskiet.al ,J. Euro.Cer.Soc., 32, pp.1983-1987,(2012).
- [3].B.C.H. Steele ,A.Heinzel, ,Nature, 414 ,pp.345–352,(2001)
- [4]. L D Jadhav, S H Pawar and M G Chourashiya, Bull. Mater. Sci., 30:2, pp 97–100, April (2007).
- [5]. K C Patil, Bull. Mater.Sci., 16,pp.533-541,(1993) .
- [6]. A.I.Y. Tok, F.Y.C. Boey, Z. Dong, X.L. Sun, J. Mat. Proc. Tech., 190, pp.217–222,(2007).
- [7]. PanduranganMuralidharan, Seung Hwan Jo, Do Kyung Kim, J. Am. Ceram. Soc., 91 [10], pp. 3267–3274,(2008).
- [8].Leow Chun Yan, Jumian Hassan et.al, World Applied Sciences Journal ,14:7 ,pp.1091-1094,(2011).
- [9]. V. S. A. K. Baral, Physica B, 404, pp. 1674–1678, (2009)
- [10] K. J. Andrew, J. Phys. D: Appl. Phys., 32, pp. R57-70, (1999).
- [11]. P. Sarkar and P. S. Nicholson, J. Am. Ceram. Soc., 72, pp. 1447–1449.,(1989).
- [12]. VaisakhanThampi, Prabhakar Rao Padalaand A. N. Radhakrishnan, New J. Chem. ,39, pp.1469-1476, (2015).
- [13]. Chitra Priya N.S, Sandhya K, Deepthi N. Rajendran, Nano trends: A Journal of Nanotechnology and its applications.; 18(3): 27-35p (2016).
- [14]. Sandhya k., Chitra Priya N.S, Aswathy P.K, Deepthi N Rajendran, Praveen Thappily, AIP conference Proceedings, 1849,020032 (2017).
- [15]. Chitra Priya N.S, Sandhya k, Deepthi Rajendran, International Journal of Engineering Trends and Technology, 37: 184-188,(2016).